Control of Propeller Cavitation in Operational Conditions

A. Vrijdag (MSc., Delft University of Technology/ Netherlands Defence Academy)
D. Stapersma (Prof., Netherlands Defence Academy/ Delft University of Technology)
T. van Terwisga (Prof. PhD., Delft University of Technology/ Maritime Research Institute the Netherlands)

Source: Royal Netherlands Navy

Off design conditions can have a severe impact on ship propulsion system behaviour. Resistance increase for instance leads to a higher engine loading, and can also easily lead to a decrease of cavitation inception speed with respect to calm water conditions. Wakefield variations due to ship motions, waves and manoeuvres also have effect on engine loading and on propeller cavitation. This paper discusses the model based development of a propulsion control system aiming at increased cavitation free time in operational conditions, while preventing engine overloading and keeping manoeuvring characteristics acceptable. The developed propulsion control system has been tested extensively in a simulation environment before full scale trials took place in February 2008. Results in terms of full scale propulsion system behaviour are presented, including photos showing the propeller cavitation behaviour in operational conditions.

KEY WORDS
Propulsion, propeller, cavitation, control, pitch, dynamics, ship, frigate, diesel engine, acoustic signature management, acceleration, deceleration, simulation, verification, calibration, validation

INTRODUCTION
Signature management is of growing importance for naval ships. Due to the stringent demands on inboard as well as outboard noise levels, increasing effort is being put into the investigation and control of noise sources, such as vibrating machinery and propeller cavitation. *Acoustic signature management* for naval vessels serves multiple goals: First of all, the risk of being detected by the acoustic sensors of the opponent (including acoustically triggered mines), greatly depends on the acoustic signature. And secondly, the own acoustic detection range is decreased by self-noise, which increases the chance of being detected before *having* detected. From full scale measurements it is known that off-design conditions have a considerable influence on cavitation performance of ships propellers, and thus on the ships acoustic signature. The effects of seastate and manoeuvring are reported in for instance Verkuyl (2000). Measurements onboard the oceanographic research vessel HNLMS Tydeman of the Royal Netherlands Navy, show that, compared to the calm water condition, the cavitation inception speed is reduced by as much as 75% in bow quartering waves, seastate 5. As can be seen in Fig 1, headwaves result in a decrease of 100%: No cavitation free speed is left for this condition. The use of 20 degrees rudder in calm seas is reported to give a decrease of as much as 55%, as can be seen in Fig 2.
A research project was started in the Netherlands, aiming at implementation of a propulsion control system that increases cavitation free time in operational conditions. To develop such a control system use is made of a ship propulsion simulation model.

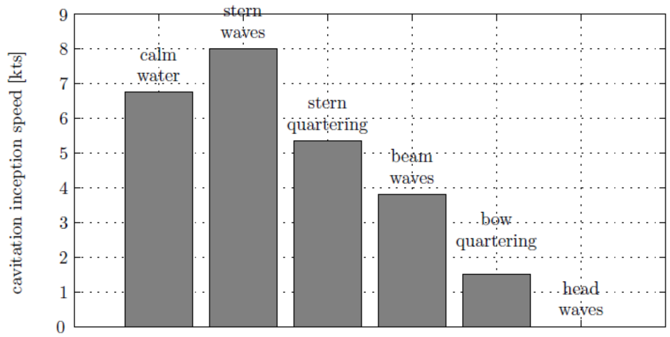

Fig 1: Effect of wave direction on Cavitation Inception Speed. Reproduced from Verkuyl (2000)

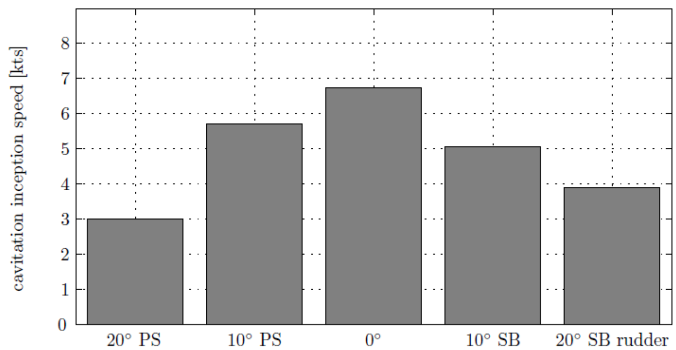

Fig 2: Effect of rudder angle on Cavitation Inception Speed. Reproduced from Verkuyl (2000)

Use of a simulation model necessitates development, verification, calibration and validation of this model. Only after these laborious tasks the simulation model can rightfully be used to make predictions instead of, or prior to measurements. The validated simulation model is used to develop and test a propulsion control system which results in improved (dynamic) behaviour of the total ship in operational conditions. Since many possible controller goals can be pursued, it is chosen to limit the practical implementation to a controller aiming at an increase of cavitation free time, while preventing thermal overloading of the engine, and keeping manoeuvring characteristics within acceptable limits. The research is further limited with respect to the type of operational conditions that are considered. Due to the immaturity of propeller cavitation prediction for ships in a turn, it is chosen to limit the current research to straight line manoeuvring characteristics. The objectives and their related research questions are summarized by:

• Create a ship propulsion simulation model that represents reality accurate enough to make it useful for controller development.
  – What is the validity of this model with respect to: propeller cavitation inception, diesel engine behaviour and straight line manoeuvring characteristics?

• Use the simulation model to develop a propulsion control system that aims at increased cavitation free time in operational conditions, and test this propulsion control system on full scale.
  – How should ship propulsion simulation models be used in order to have maximum benefit during development and testing of a practically applicable ship propulsion control system?
  – How should a newly developed propulsion control system be tested in order to asses its performance?

• Investigate the effects of operational conditions on the performance of the propulsion system.
  – What is the effect of acceleration and deceleration on the system performance?
  – What is the effect of added resistance (due to for instance wind or fouling) on the system performance?
  – What is the effect of waves on the propulsion system performance?

In February 2008, the cavitation-reducing propulsion control system was tested full scale, onboard a frigate of the Royal Netherlands Navy (RNLN). The goal of these trials was to demonstrate the effect of the developed new propulsion control system on the propulsion system in general and on propeller cavitation in particular. A comparison with the existing propulsion control system was also made. Time- synchronized measurements of both engine and propeller variables were made, including high- speed video recordings of the propeller.
This paper gives a brief overview of the various activities that led to the temporary implementation of the propulsion control system, and presents some of the full scale trial results.

THE SIMULATION MODEL

The goals that are pursued with the model are the basis for the simulation model development. In this case the goals are set as follows:
The ship propulsion simulation model should represent reality accurate enough to make it useful for the development of a propulsion controller. This controller should aim at increasing cavitation free time in operational conditions by active control of both shaft speed and propeller pitch. The model should also give accurate enough output to enable judgment of diesel engine loading and straight line manoeuvring characteristics.
This abstract goal includes the somewhat vague descriptions ”accurate enough”, ”useful”, and ”operational conditions”. To come to clear specifications of the simulation model an interpretation of the high level goal is made here:

- *Create a model containing the following sub-models: engine-, propeller-, gearbox- and manoeuvring model.*
- *Accuracy of the propeller model should be such that conclusions with respect to propeller cavitation can be drawn.*
- *Accuracy of the diesel engine model should be such that the currently used engine overloading-criterion of the diesel engines can be checked.*
- *Accuracy of the manoeuvring model should be such that conclusions with respect to straight line manoeuvring behaviour can be drawn.*
- *The model should accommodate for the simulation of increased ship resistance and fluctuating wakefield.*

- *Accuracy of the CPP hydraulic system should be such that it gives good performance predictions for true continuous variation of the propeller pitch.*

Although these specifications are still somewhat vague, at least they give a starting point for setting up the simulation model. Whether the resulting total simulation model gives outputs with sufficient accuracy cannot easily be said beforehand due to uncertainty propagation through the various sub-models. A mathematical approach to uncertainty propagation through various coupled sub-models is discussed in Vrijdag et al. (2007) and Schulten and Stapersma (2007).

The various phases in the development of the simulation model that was used in this research project are illustrated in Fig 3. Through analysis of the existing ship and its propulsion plant, a conceptual model is formed. The model qualification should ensure that the conceptual model is adequate for the intended application. This conceptual model is then programmed, after which it is verified whether the simulation model represents the developer's conceptual description of the model. After successful verification, the simulation model can be calibrated to increase the agreement between model and reality. Finally validation should lead to a quantified level of agreement, which should give the user some idea of the expected accuracy of predictions. In this paper reality is briefly described, after which the general structure of the validated model is presented. Although extensive verification, calibration and validation activities took place, they are not reported here.

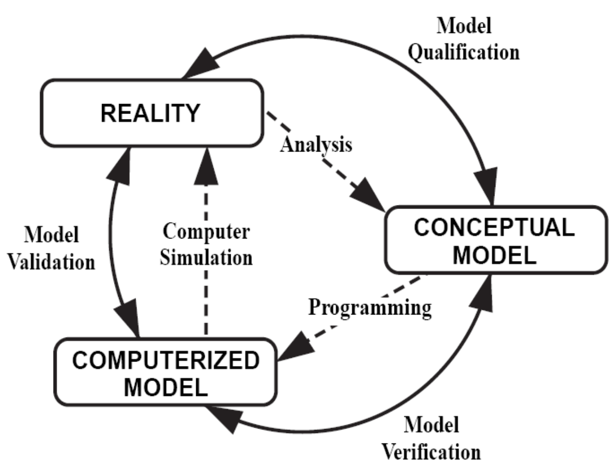

Fig 3: Development cycle of a simulation model. (Schlesinger, 1979)

The Ship Propulsion System that is to be modelled here is based on the Multipurpose Frigate (M-frigate) of the Royal Netherlands Navy. This ship- type is chosen since early on in the project it was decided that full scale trials were to be carried out onboard an M-frigate. The layout of the propulsion system of the M-frigate is shown in Fig 4, with some general data given in Table 1. The ship is approximately 120 meters long and 14 meters wide, and has a displacement of ≈ 3300 tons. It is a twin shaft ship, with both shafts linked to a dedicated CODOG installation. The 4-stroke turbocharged diesel engines run in the medium speed range (< 1000rpm), and are capable of propelling the ship up to speeds of ≈ 20 kts. Two Rolls Royce gas turbines are capable of driving the ship up to ≈ 29 kts in calm water conditions. Both shafts are fitted with a 5 bladed Controllable Pitch Propeller (CPP) rotating inward over the top. These propellers have been optimized for high Cavitation Inception Speed (CIS) and for high propeller efficiency. Two inclined rudders are fitted directly behind the propellers, capable of roll-reduction by continuous active rudder adjustments.

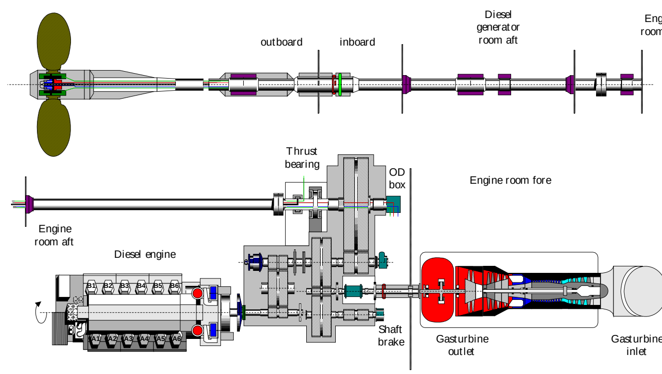

Fig 4: The ship propulsion plant. [Source: RNLN]

Table 1: General ship data.

Type of vessel	Frigate
Lpp	114 m
Engines	Stork - Wärtsilä Diesel SW280
Number of propellers	2
Displacement	~3300 tons

The propulsion system of the M-frigate can be operated in various configurations. Apart from a Diesel Engine (DE) or Gas Turbine (GT) driven shaft, it is also possible to sail with one non-driven shaft which is beneficial during maintenance on one shaft line, or during prolonged operation at low ship speed. This non-driven shaft can be chosen to run freely at low rotating speed (trailing), or can be locked by a shaft brake. In the latter case the propeller is often feathered to reduce resistance.

Only the double DE configuration is to be simulated with the ship propulsion simulation model, while GT operation is not required. This is a choice that is based on the goals that are pursued with the model. DE's put more constraints on the propulsion controller that is to be developed. This is expected to lead to better understanding of the balancing between engine loading, propeller behaviour and manoeuvring characteristics. Furthermore the ship speed at which gains in cavitation free time are expected lies in the DE operating range. Prolonged GT operation during the full scale testing period was considered too expensive considering the low fuel efficiency of the GT at relative low ship speeds. It is acknowledged that the need for increased cavitation free time also holds when sailing on GT's. It is expected that findings of this project can also be used for further development of a “silent” control system for a gas turbine-driven ship.

The Validated Model that is used in this project, is schematically shown in blockdiagram form in Fig 5. This figure shows the various submodels and their boundaries, and uses the notation as introduced in Vrijdag et al. (2007). The variables that link the various submodels are called the linking variables and are noted as $\mathbf{y}_i$, submodel parameter inputs are denoted as $\mathbf{x}_i$, while parameters that are input to multiple submodels are denoted as the shared variables $\mathbf{x}_s$. Outputs of submodel i are indicated by $\mathbf{z}_i$. This systematic approach proved valuable during the project, especially in calibration and validation.

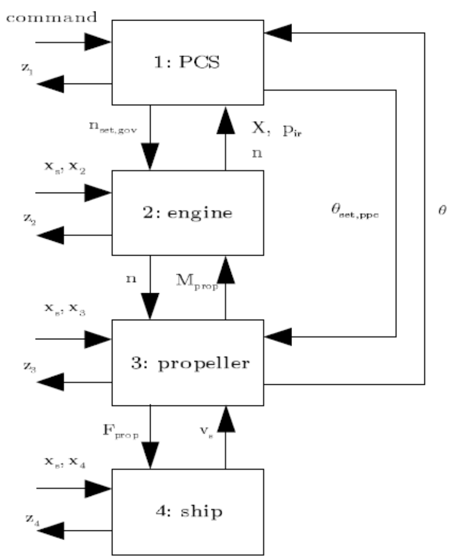

Fig 5: Schematic overview of the conceptual model.

The Propulsion Control System (PCS) is the top sub-model that is shown in Fig 5. Based on the command given by the user, and various plant measurements, the PCS gives an engine speed setpoint to the Diesel Engine (DE) –governor $n_{set,gov}$, as well as a pitch setpoint to the low level Propeller Pitch Controller (PPC), denoted by $\theta_{set,ppc}$. Especially during transients the PCS bases its two setpoint outputs on the measurement of the fuelrack setting X, inlet receiver pressure p_{ir}, actual pitch θ and actual shaft speed n.

The engine submodel includes more than just the engine: it includes the governor, the actuator, the high pressure fuel pumps, the engine itself, the gearbox and the shaft dynamics. The governor is modelled, according to manufacturer data and onboard settings, as a PI-controller with fuelrack limitation based on engine speed. The actuator is a first order linear transfer function, and the high pressure fuel pumps are modelled by means of a lookup table with fuel injection per cycle based on shaft speed n and fuelrack setting X.
The engine itself is also modelled by lookup tables that are available within the RNLN since the M-frigate propulsion plant has often been analysed in the past. The engine output p_{ir} is also a model output, based on lookup table output.
The gearbox is modelled by a simple gearbox ratio, and with a constant gearbox efficiency factor. Shaft dynamics are modelled as

$$n(t) = \frac{1}{2\pi \cdot I_p} \int_0^t \sum M dt + n_0$$

where n is the shaft speed (having initial value n_0 at time $t=0$), M is the sum of all torques working on the rigid shaft and I_p is the effective rotational inertia of the shaft system (engine and gearbox rotating parts, shaft, propeller and entrained water, all considered constant).

The propeller submodel includes the low level Propeller Pitch Controller, the hydraulic pitch actuating system, the openwater diagram of the propeller, and a simple wakefield model. Without giving all details, the basics of use of the openwater diagram are given by:

$$J = \frac{v_s(1-w)}{nD}, \; k_t = f(\theta, J), \; k_q = g(\theta, J),$$

$$M_{prop} = \eta_r \cdot k_q \rho n^2 D^5, \text{ and } F_{prop} = k_t \rho n^2 D^4$$

Further details on the modelling details of the hydraulics and the Propeller Pitch Controller (PPC) are not given here.

The ship submodel includes the ship resistance curve, including the possibility to add extra resistance, and the ship dynamics. The resistance curve is taken from model-tests, and given by: $R = h(v_s)$. The effect of resistance increase due to propeller action is modelled by $F_{ship,0} = \frac{R}{1-t}$, with t being the thrust deduction factor from model tests. Further resistance increase is possible by addition of two calibration factors :

$$F_{ship} = \alpha_R F_{ship,0} + R_0$$

Dependent on the source of the extra resistance the two factors can be used.
Longitudinal ship dynamics are modelled as

$$v_s(t) = \frac{1}{m} \int_0^t \sum F dt + v_{s,0}$$

where v_s is ship speed (having initial value $v_{s,0}$ at time $t=0$), F is the sum of all forces working in the longitudinal direction of the ship and m is the effective mass of ship including added mass which are both assumed constant.

DEVELOPMENT OF THE PROPULSION CONTROL SYSTEM AIMING AT INCREASED CAVITATION FREE TIME

The goal of a simulation model is to make predictions of real life system behaviour. In this specific case interest goes out to predictions of real life system behaviour if a specialized propulsion control system (PCS+) is applied instead of the currently applied PCS (of which a copied version is part of the validated model presented in the previous section). The plant model, in which the authors have confidence substantiated by the validation process, has been used to develop and test a PCS+ in a simulation environment before actual full scale trial took place. Even the formal factory acceptance tests (FAT's) of the PCS+ by technical staff of the RNLN were carried out with the use of the simulation model. In this section the basic ideas behind the newly developed PCS+ are dealt with.

The goal of the newly developed PCS+ is as follows:

The PCS+ should aim at increasing cavitation free time in operational conditions by active control of both shaft speed and propeller pitch. It should prevent overloading of the diesel engine, and should ensure acceptable straight-line manoeuvring characteristics.

As shown in Fig 6 there are many combinations of shaft speed and pitch that result in the same ship speed. The choice for one of these combinations, both in static as dynamic conditions, is a compromise between various goals that one pursues with the ship, limited by engine loading and manoeuvring criteria.

The figure also shows the virtual shaft speed, which is a variable that is used in (onboard) practice to communicate the propulsion setpoint. It is defined by: $n_{virt} = \dfrac{\theta - \theta_0}{\theta_{nom} - \theta_0} \cdot n$, where θ_0 and θ_{nom} indicate zero-thrust pitch and nominal pitch.

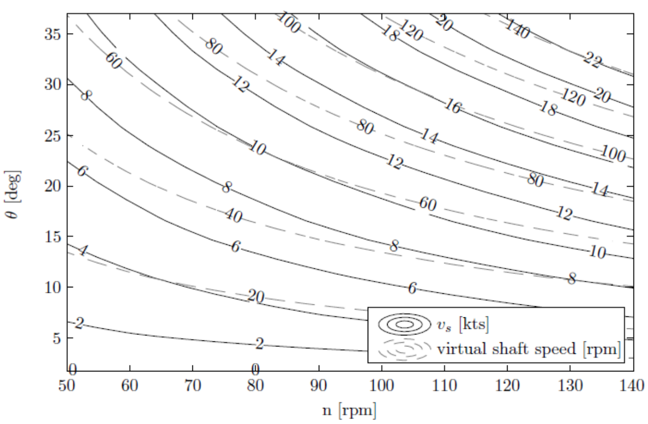

Fig 6: Contours of ship speed and virtual shaft speed in the shaftspeed-pitch plane.

In the discipline of propeller hydrodynamics it is customary to present cavitation inception behaviour of a propeller in a propeller inception diagram. This is a diagram showing the dimensionless cavitation-number σ_n versus the thrust- or torque coefficient (k_t or k_q) or versus the advance ratio J. σ_n is a non dimensional measure of the potential of the propeller to cavitate, and is given by:

$$\sigma_n = \frac{p_0 - p_v + \rho_{sw} g z}{\frac{1}{2} \rho_{sw} n^2 D^2},$$

where p_0 is the atmospheric pressure, p_v is the vapour pressure of seawater, ρ_{sw} is the density of seawater, g the gravitational acceleration, and z the water height above the propeller shaft. n represents shaft speed, and D is the propeller diameter.

Inception conditions are drawn to show the locus of propeller working points where a specific type of cavitation starts. Due to their shape the inception lines are often related to as the "inception bucket". An example is shown in Fig 7. Note that a nominal ship operating line is also shown. Operating on the left hand of this bucket-shape will result in pressure side cavitation, while operation on the right hand side will in this case results in tip-vortex suction side cavitation. Unfortunately this bucket only holds for one single pitch angle. A change in pitch results in (a) a shift in location of the bucket with respect to k_t and (b) a different shape of the bucket and thus requires a completely new diagram. The same holds for buckets that are presented on basis of k_q or J. The shift in bucket is illustrated for three different model scale pitch angles (indicated by 0, -6.7 and -12.1 deg) in Fig 8.

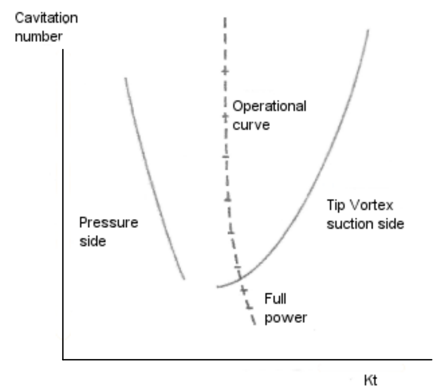

Fig 7: Example cavitation bucket showing two inception lines

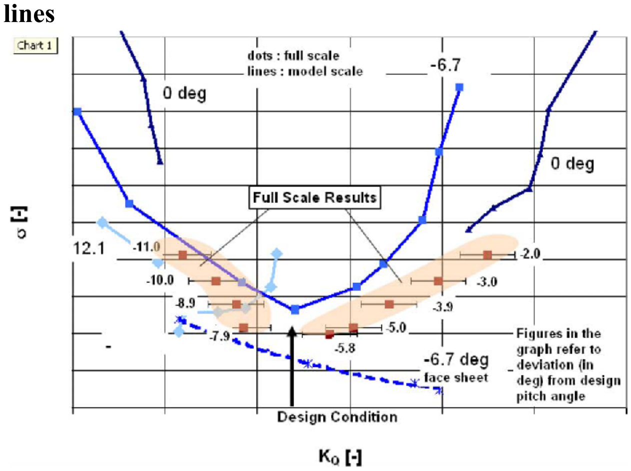

Fig 8: Comparison of full scale visual cavitation inception with similar results from model tests in the Depressurised Towing Tank, the latter extrapolated to full scale values. Source: van Terwisga et al (2007).

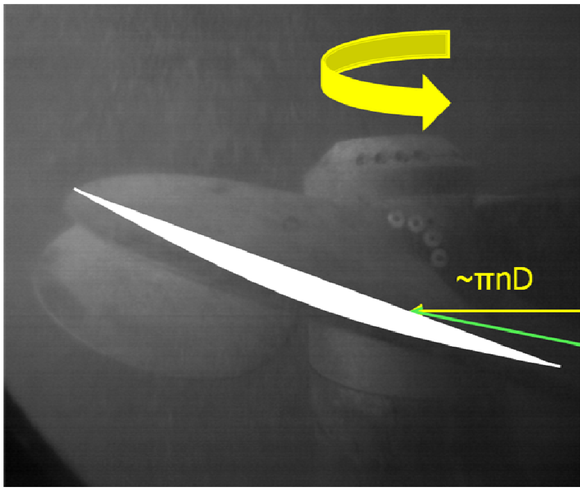

Fig 9: Velocity triangle on full scale.

In this paper an alternative presentation of the inception diagram is presented where the variable k_t is replaced by an effective angle of attack of the flow encountering the blade, The effect is that a change in pitch angle will practically not result in a shift of the bucket. This type of presentation is useful both during analysis of propeller design but even more in the design phase of a propulsion controller.

The idea is as follows: cavitation takes place if the pressure somewhere around the propeller blades drops below the vapour pressure. The pressure distribution around the blades is dependent on the (local) inflow angles of the propeller sections. These inflow angles are the result of shaft speed, ship speed, wakefield, and the propeller geometry. This is illustrated by the vector diagram that is superimposed on the picture of a full scale propeller, photographed through a window in the hull, as shown in Fig 9. It is immediately acknowledged that this simplified representation does not take into account aspects such as variations in velocity field during a revolution, dynamics in hydrodynamic circulation, and induced velocities due to propeller loading. Nevertheless the figure does illustrate the main aspects that determine cavitation inception conditions.

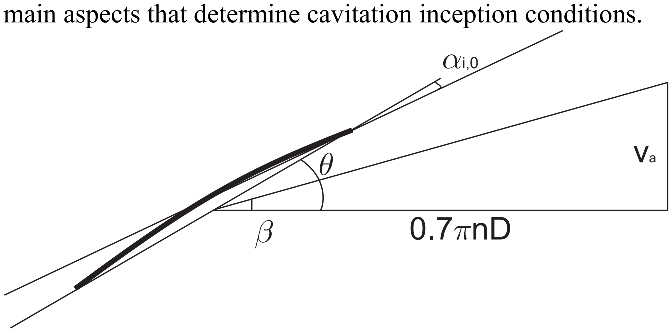

Fig 10: Schematic sketch of velocity triangle at r=0.7R.

From Fig 10 it can be derived that the local inflow angle contains pitch θ, flow angle β and a correction for the shock free entry angle α_i as follows:

$$\alpha_{eff} = \theta - \beta - \alpha_i$$

Working this out gives:

$$\alpha_{eff} = \underbrace{\arctan\left(\frac{P_{0.7R}}{0.7\pi D}\right)}_{\theta} - \underbrace{\arctan\left(\frac{c_1 v_a}{0.7\pi nD}\right)}_{\beta} - \alpha_i \qquad (1)$$

where c_1 is a correction factor that can be used for calibration. α_i is the shock free entry angle that is dependent on geometry (camber) and on induced velocities near the leading edge.

For now only the geometric (camber) part $\alpha_{i,0}$ of α_i is determined and incorporated in the effective inflow angle estimation process. $\alpha_{i,0}$ is calculated from the (pitch dependent) camber c and thickness f and given without derivation:

$$\alpha_{i,0} \approx \frac{c f_{max}}{c^2/4 - f_{max}^2}$$

The alternative presentation of the inception bucket that is used here, is in fact nothing more than a mapping from one space to another. This mapping is visualised in Fig 11, where the transformations H and G are well known operations using the open water propeller diagram. Their inverse operations can sometimes pose numerical problems since for one single value of k_t/ k_q the advance ratio J is not always unambiguously defined. For the propeller under consideration the operations H^{-1} and G^{-1} were possible for positive pitch angles in the first quadrant.

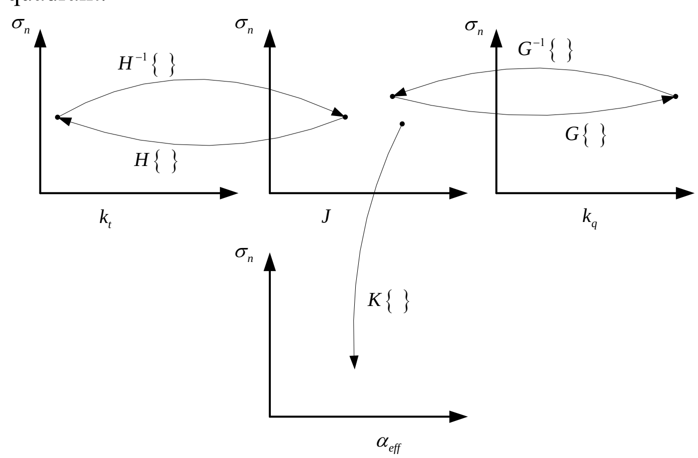

Fig 11: Various presentations of the inception bucket, and transformations between them.

Transformation K is defined by equation (1), with a freedom in the calibration parameter c_1. The calibration of c_1 is closely related to the ultimate goal of the α-bucket: one single bucket that holds for a big range of pitch angles.

In this project three full scale observed cavitation buckets (k_q-buckets, each observed at a different pitch angle) were used to determine the coefficient c_1 such that the best overlap of the three buckets in the α_{eff} versus σ_n plane is found. Other ways to calibrate the transformation might include use of model scale results or computational predictions.

The α-bucket presentation serves multiple goals: first of all it allows for predictions of the cavitation inception bucket for pitch angles that were not used during the calibration. Secondly, as will be shown, this presentation can be used onboard to keep the propeller operating point in the middle of the α-bucket during operational conditions.

The latter necessitates continuous online estimation of α_{eff}, based on available measurements. Onboard sensors of the ship under consideration allow for estimation of the operating point in both the σ_n-k_t and the σ_n-k_q plane. Via the transformation K shown in Fig 11, these points can be transformed to the σ_n-α_{eff} plane. Comparison of this estimated operating point with the derived α-bucket gives an indication of the margin against cavitation that is present.

In the new PCS, the actual effective angle of attack α_{eff} is continuously estimated, and compared to the desired angle of attack $\alpha_{eff,set}$, that is chosen in the middle of the α-bucket. If there is difference between the two, a propeller pitch change is ordered by the PCS+ to recover to the desired angle of attack. This is an immediate action that for instance results in wave frequent propeller pitch actuation.

To ensure that a persistent pitch increase or decrease (due to for instance high resistance conditions) does not lead to a performance degradation in terms of decreased or increased sustained ship speed, the shaft speed is slowly adjusted in order to arrive at the requested virtual shaft speed contour shown in Fig 6, which has an intuitive relation with ship speed.

Further examples on the use of the variable α_{eff} can be found in Vrijdag(2008).

THE FULL SCALE TEST SETUP

During the full scale trials the PCS of the starboard shaft line was temporarily bypassed, so that actual control took place by an industrial processor board, that could easily be reconfigured with a different control system. Data logging took place via the same industrial processor board, as well as on multiple other systems. Two viewing windows above the starboard propeller were mounted with high speed video cameras, which via a pulse-signal could be time- synchronised with the rest of the measurements.

The hull plates above both the starboard and the port propeller were fitted with accelerometers, which were used as a secondary system to determine whether cavitation was present. The advantage of these sensors is that they can detect cavitation that is not visible from the windows. On the other hand they do not tell where the cavitation occurs, so that it cannot be distinguished whether the noise comes from the propellers or from another cavitation part such as the rudder or the strut. Due to the propagation of the cavitation noise through the water and the hull, the port and starboard signal are highly correlated, which further complicates the analysis. In certain conditions however, these sensors can help in the analysis of the trial results, as will be shown in the discussion of the full scale acceleration trial.

Fig 12: Diver cleaning the viewing window above the propeller.

FULL SCALE RESULTS

To test the performance of the new developed propulsion control system, full scale trials were carried out onboard HNLMS van Galen, in February and March 2008. The operating area was the Caribbean Sea, where the ship was deployed at that time. The system performance using the PCS+ is compared with the system performance when using the existing propulsion control system. Where considered useful or necessary to increase understanding use is made of extra simulation predictions. Such predictions can be used instead of measurements that where not carried out, and can be carried out under exactly the same conditions, so that external disturbances due to for instance waves do not contaminate the output variables.

The experiments that were planned and communicated with the ships crew were described in a test-protocol. This protocol contained various types of tests that were designed with the goals of the project, as defined earlier, in mind. The relevant goals and research questions that led to the test-protocol are repeated here:

- Use the simulation model to develop a propulsion control system that aims at increased cavitation free time in operational conditions, and test this propulsion control system on full scale.
- Investigate the effects of operational conditions on the performance of the propulsion system
  - What is the effect of acceleration and deceleration on the system performance?
  - What is the effect of added resistance (due to for instance wind or fouling) on the system performance?
  - What is the effect of waves on the propulsion system performance?

It is chosen to discuss only the acceleration test in this paper: To investigate the effect of acceleration on the system behaviour, multiple acceleration tests were defined. The helmsman was asked to limit the use of rudder to preferably <5 degrees, and the roll-damping system was switched off.

The tests were carried out by both the existing and the new PCS driving the starboard shaft. The portside shaft was continuously driven by the old PCS. During the test period prevailing easterly winds were encountered, increasing in strength from 3 to 5 Beaufort, resulting in seastate 3 to 4. No calm water conditions where found, so that calm water system behaviour could not be fully separated from the disturbing wave induced system behaviour. To make the comparison as fair as possible, the importance of keeping the same course for a prolonged period (during the comparison tests) was emphasized onboard. During most of the tests this was possible, but as might be expected from a field experiment, in specific cases the conditions necessitated alteration of course, resulting in a less fair comparison.

The acceleration test will reveal the benefits with regards to cavitation reduction and with regards to acceleration time.

Since it is not possible to elaborate on all accelerations and decelerations that have been carried out, only an acceleration from ≈10kts-14kts is dealt with here. The most important graphs are shown and discussed, together with various photographs of the starboard propeller, taken with the high speed video camera's. To make a comparison possible, all graphs contain measurements of the same manoeuvre, carried out by both the old and the new PCS driving the starboard shaft.

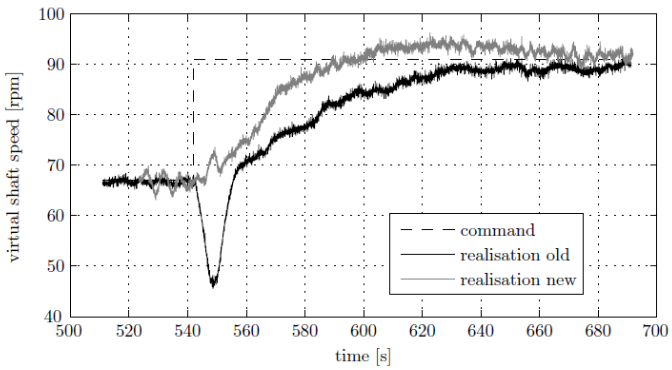

Fig 13: Command and virtual shaft speed.

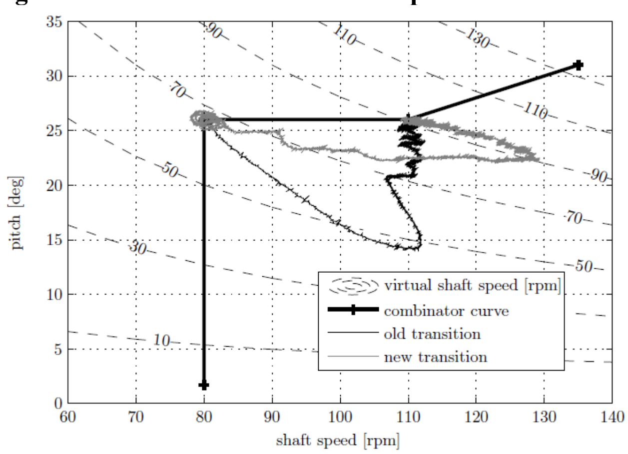

Fig 14: Trajectory in the n-θ plane.

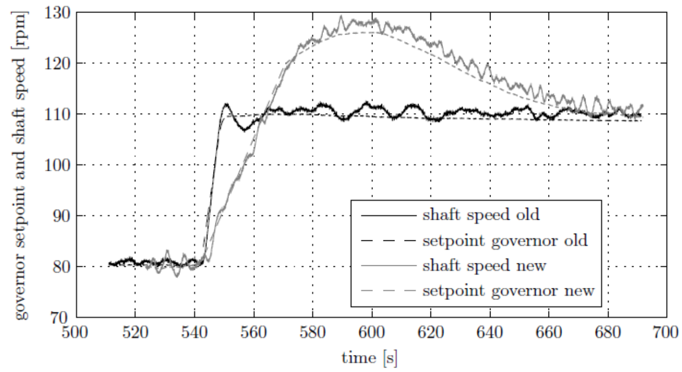

Fig 15: Scaled down governor setpoint and shaft speed.

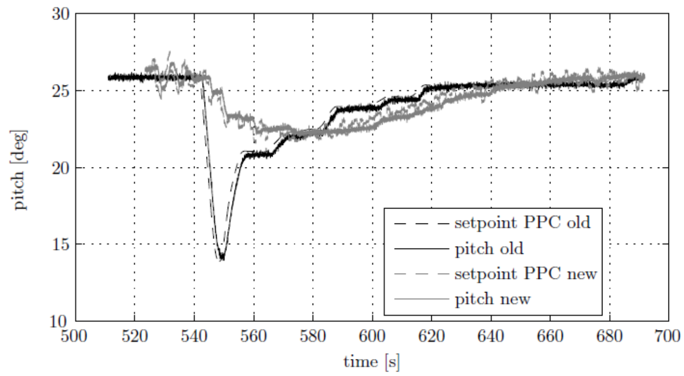

Fig 16: Setpoint pitch and pitch.

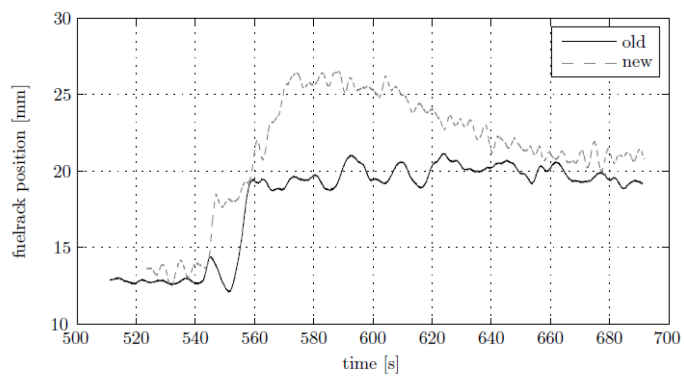

Fig 17: Fuelrack position.

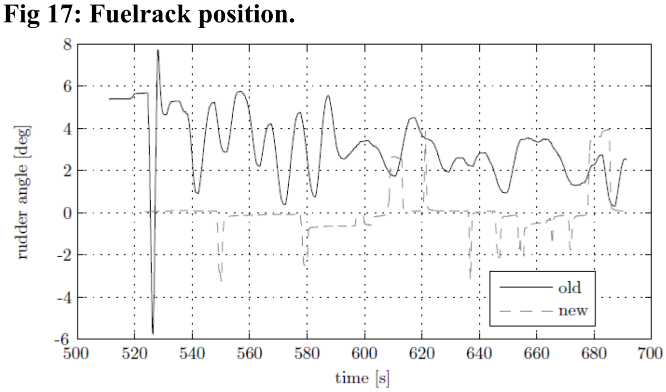

Fig 18: Rudder angle.

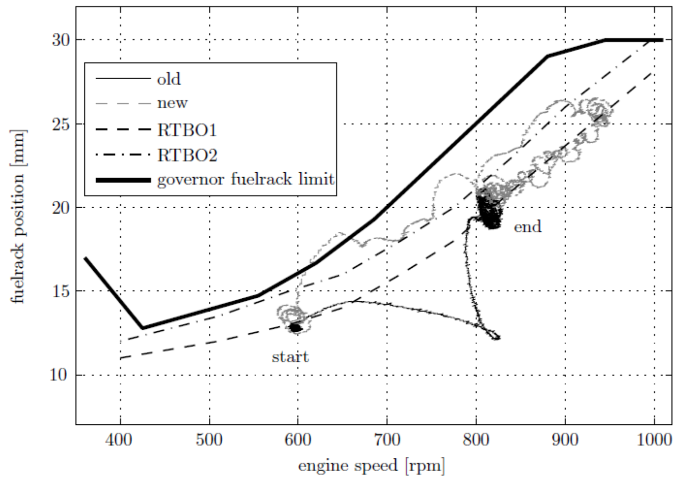

Fig 19: Engine diagram.

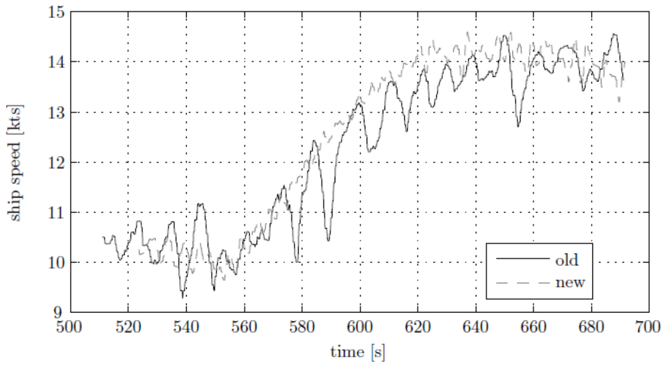

Fig 20: Ship speed.

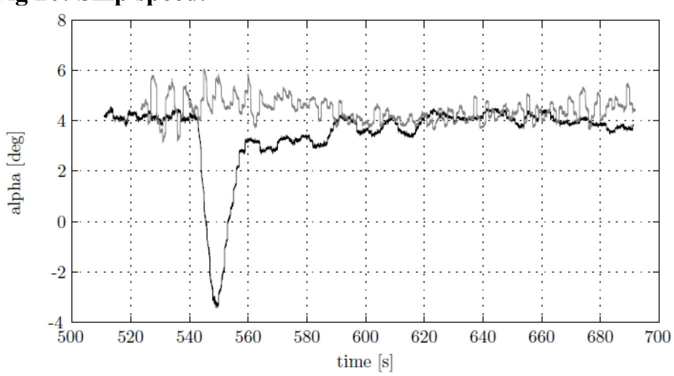

Fig 21: Effective angle of attack.

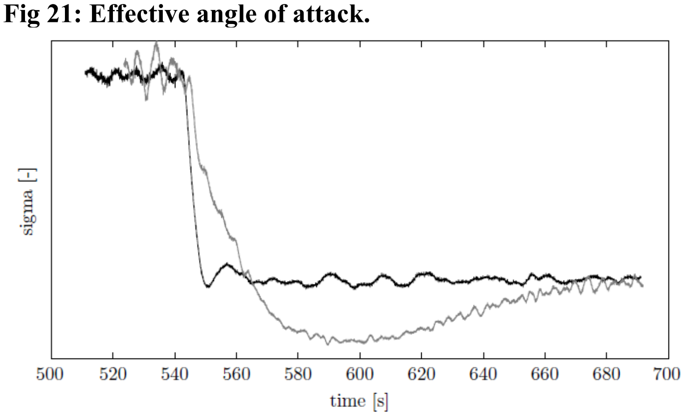

Fig 22: Cavitation number.

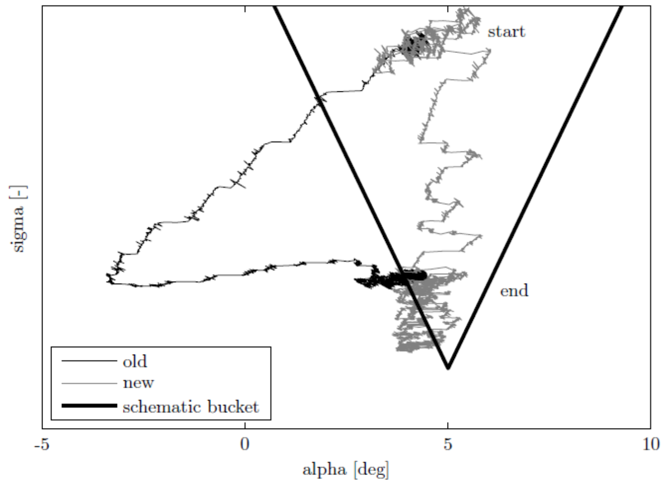

Fig 23: Trajectory in the α-bucket.

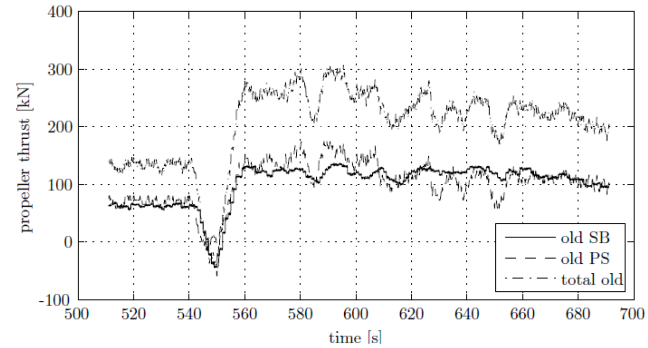

Fig 24: PS and SB thrust of the old PCS.

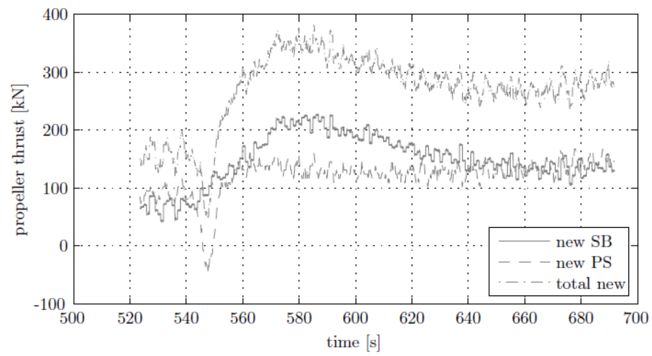

Fig 25: PS and SB thrust of the PCS+.

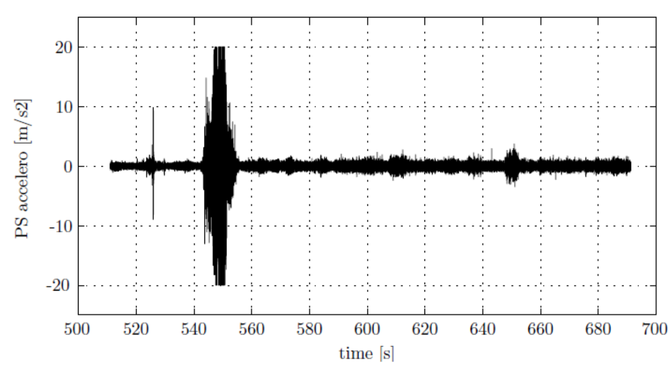

Fig 26: Acceleration signal above the portside shaft. Old PCS.

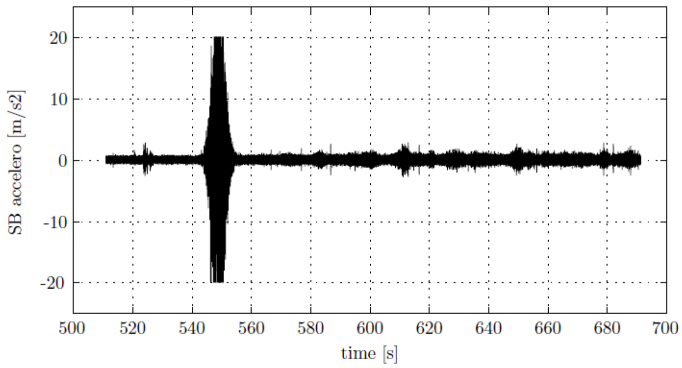

Fig 27:Acceleration signal above the starboard shaft. Old PCS.

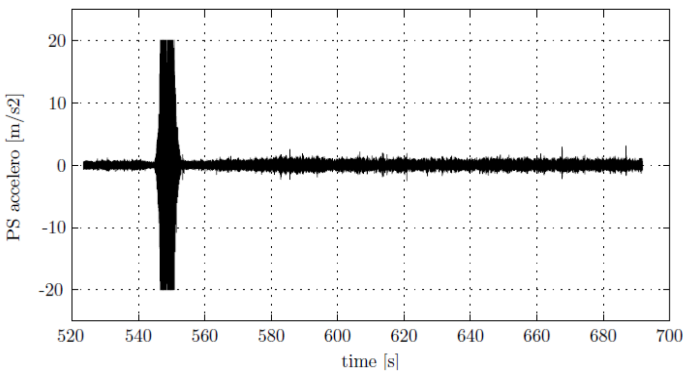

Fig 28: Acceleration signal above the portside shaft. PCS+.

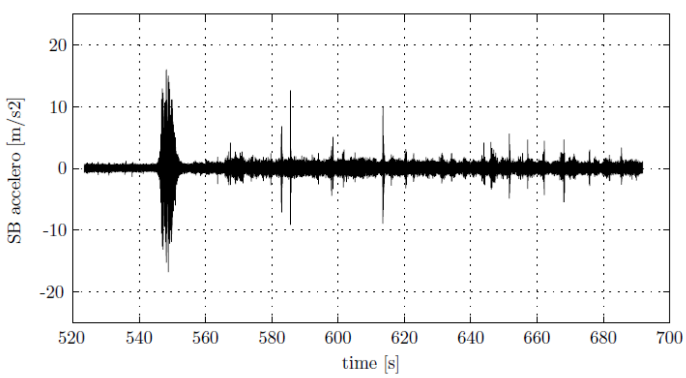

Fig 29: Acceleration signal above the starboard shaft. PCS+.

To give the discussion some structure it is chosen to split it up into separate discussion of the aspects ***propeller behaviour***, ***engine behaviour***, and ***manoeuvring behaviour***:

Propeller Behaviour

Old PCS: As can be seen in Fig 14, the static propeller pitch operating point at both the beginning and the end of the transient lies at 26 degrees as fixed by the combinator curve. The active pitch reduction that is ordered by the PCS reduces the pitch to ≈14 degrees in order to reduce the engine loading. Fig 24 shows that the net effect of the active pitch reduction and the shaft speed increase results in a steep drop of propeller thrust. Between t=542-555s, total thrust drops below the value necessary to maintain the original speed. Between t=546-551s the total thrust even becomes negative, which means that the propellers are acting as brakes.

The shaft speed reaches its setpoint around t=550s. The PCS now starts to increase the load by slow increase of the low level propeller pitch setpoint, followed by the pitch as shown in Fig 16. Up to t=557s this pitch increase is quite fast, until the Reduced Time Between Overhaul (RTBO1)-line of the PCS is crossed (Fig 19). The PCS now takes action by decreasing the pitch-rate, in order to prevent an overshoot across the RTBO2-line. From now on the pitch is allowed to increase with a rate that is dependent on the loading of the engine: due to a net resultant longitudinal force, the ship accelerates, resulting in a decrease of engine loading. Pitch is increased slowly, and the ship speed increases further, and so on. Dependent on the actual conditions the propeller pitch is increased until the combinator value is reached. If engine loading is too high (due to for instance high ship resistance), pitch remains constant at a reduced value, leaving the operator command only partly effectuated, resulting in an unnecessarily decreased ship speed.

The path through the α-bucket is shown in Fig 23. The aggressive pitch reduction results in a significant drop of angle of attack, which, as will be shown later, leads to pressure side cavitation due to under-loading of the propeller. Subsequently, pitch is increased fast, resulting in a quick recovery of angle of attack. After that, pitch increases gradually in such a way that α_{eff} stays approximately constant (Fig 21). The starboard cavitation behaviour is shown in Fig 31, where various photos taken during the manoeuvre are shown with intervals of 1s, starting at t=540s. Note that at the top of each photo the leading edge of the rudder is visible. The (visual) inception point lies between 543-544s. The aggressive pitch reduction clearly results in significant pressure side vortex cavitation, which stays visible for ≈10s. This agrees with onboard experience: during an acceleration, high levels of vibration and noise are often observed in the aft-ship. The most significant cavitation is observed around t=549-550s, which agrees with the lowest α-value found in Fig 21 and the most western point of Fig 23.

The measured acceleration signals above the port and starboard shaft are shown in Fig 26 and Fig 27. Around t=543s the acceleration signal amplitude of both sides suddenly increase up to the maximum sensor value. The interval of increased acceleration levels aligns well with the visually observable cavitation.

PCS+: Fig 14 and Fig 16 show that active pitch reduction is still applied by the PCS+, albeit a lot less aggressive. As dictated by the PCS+, the pitch is constantly adjusted with the goal of keeping the estimated effective angle of attack α_{eff} at the setpoint $\alpha_{eff,set}$ that is set in the middle of the α-bucket. The resulting path in the bucket is presented in Fig 23, showing less fluctuations in α_{eff} than in the "old PCS"-case, which is likely to result in favourable cavitation behaviour. On the other hand the new PCS temporarily operates at higher shaft speed, and thus lower in the bucket.

The cavitation behaviour of the starboard propeller is shown in Fig 32 starting at t=543s. Due to lighting conditions as well as a course change more air bubbles are visible underneath the ship. Except for a small traces of vortex cavitation around t=552s, no cavitation is observed. Due to limited video- recording time a considerable part of the manoeuvre (after t=557s) is not captured on video. Therefore, it might be questioned whether cavitation occurred at later times, for instance during the shaft speed of 130rpm around t=595s, or during the high thrust interval around t=580s. This question can be answered by making use of the accelero-signals measured above the port and starboard propeller. Both the port and the starboard sensor output are shown in Fig 28 and Fig 29, both showing considerable excitation of the sensors around t=550s. However, based on the photos taken around that time, it is concluded that this excitation must be caused by aggressive pitch reduction of the portside propeller. This is supported by the lower excitation of the starboard sensor. When we now consider the time-interval 560-700s, where no photos are available, the starboard acceleration-signal shows only a small increase with few very sharp peaks, indicating that the high shaft speed of the starboard side caused no or only very little cavitation. Drawing very strict conclusions based on the acceleration signals remains difficult, since the sensors do not tell the source of the vibration.

Engine Behaviour

The trajectory in the engine diagram is quite different for the old and the new PCS. The dip in loading of the old PCS during the acceleration indicates that the engine is over-protected, which was shown to result in a temporary deceleration of the ship. Around t=560s the old PCS has increased fuelrack up to RTBO1, after which the pitch rate is decreased in order to keep the operating point outside the RTBO2 area.

The PCS+ was shown to have only little pitch reduction. Instead, pitch is actively controlled to maintain the α at its setpoint. During the up-hill transient, the operating point follows the RTBO2-line, up to the high shaft speed of ≈130 rpm. From there on, with increasing ship speed, the balance between pitch and shaft speed is gradually found to lie more to the pitch-side.

The amount of fuelrack that is necessary to accelerate the shaft can easily be lowered by changing the desired shaft-acceleration rate in the PCS+. This will however have its consequence on the acceleration of the ship. The effect of changing the shaft-acceleration-rate parameter can easily be tested by making use of the simulation model.

Manoeuvring Behaviour

Before a comparison of the acceleration capability of the "old" and the "new" PCS is made, focus is put on possible disturbances that might affect the acceleration performance. Inspection of Fig 18 shows that during the "old" test the autopilot was used, resulting in small fluctuations in rudder angle. The mean rudder angle differs approximately 3 degrees between the runs. Although this decreases the quality of the comparisons, no serious effect is expected.

Furthermore, as can be seen in for instance the ship speed signal in Fig 20, the ship speed fluctuations (or better: the water speed as measured by the EM-log) shows a difference in frequency content during the run. Due to operational circumstances the ship had to change course between the comparison-runs. Based on the encounter frequency as derived from the speed figure, it is concluded that the "new" run was carried out in bow-quartering or bow waves, while the new run was most probably carried out in stern-quartering or stern waves. This course change would also explain the difference in total propeller thrust as shown in Fig 24 and Fig 25. Unfortunately the GPS-log computer failed during the runs, and no exact course or heading information is available.

With the mentioned disturbances in mind, a comparison between the acceleration capabilities of the two systems can only be made in a qualitative sense. Due to the course change the new PCS has a disadvantage due to the extra resistance. Despite this resistance increase the measured acceleration time seems to have been shortened by the new controller. This is expected to improve even further if not only the starboard shaft, but also portside would be controller by the new PCS. This test was however not possible since the portside was not fitted with the PCS+. To enable a fair comparison between the acceleration capabilities of both systems, two predictions of this manoeuvre are carried out. The first prediction is about the acceleration when both port and starboard are controlled by the old PCS. The second prediction is on the (non measured) behaviour when two shafts are controlled by the PCS+. Results are shown and compared to measurements in Fig 30. The comparison between the predicted and measured (PS+SB old) data, is in fact a new validation case, giving extra information on the agreement between measurement and simulation. With this new qualitative validation-information in mind the prediction on the complete new PCS-case is trusted to give a correct behaviour, although the absolute acceleration may be on the optimistic side. The new case (PS+SB new) gives an overshoot in ship speed which can be explained by the structure of the PCS+. Due to the absence of disturbing waves the small dip in ship speed at the beginning of the acceleration by the two old PCS's is clearly made visible. The possible gain in acceleration speed is also made visible.

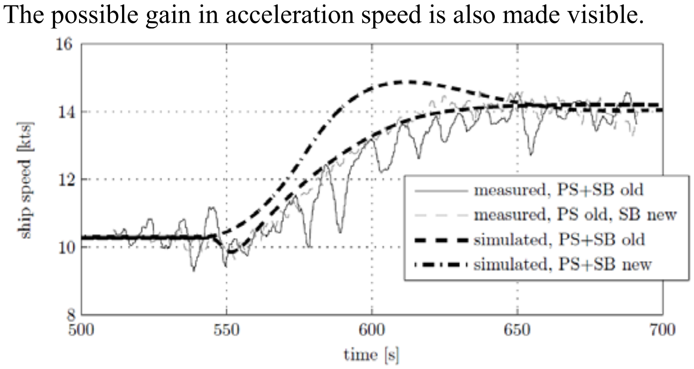

Fig 30: Measured and predicted acceleration behaviour.

This small example of ship acceleration prediction is a demonstration of true symbiosis between measurement and simulation. Only through such symbiosis it is possible to make high confidence predictions of complex multidisciplinary system behaviour.

CONCLUSIONS

A simulation model of a ship propulsion plant has been developed. From the validation phase that was not presented in this paper it was concluded that the model is adequate for development and testing of a new propulsion control system. This PCS+, aiming at increased cavitation free time in operational conditions was developed, and tested on full scale.

The limited full scale results that have been presented here show a significant increase in cavitation free time during acceleration. The engine loading is higher during the transient, but is still acceptable, considering the time-extent of the high load. With the help of extra predictive simulations, the manoeuvring capability was shown to have increased. It was shown that the increase of acceleration capability becomes significant if not one, but two shafts are driven by the PCS+.

On the whole it is concluded that model based ship propulsion controller development is very well possible, and can lead to improved system behaviour. As shown, it is even possible to increase propeller cavitation free-time by application of a specialised PCS.

In the long run, the model based development of specialised propulsion controllers for specific missions/ goals is expected to lead to a more effective use of propulsion installations. It is however strongly recommended to only trust outcomes of any simulation model after it has been verified, calibrated and validated at a level that is justified by the development phase of the propulsion installation.

ACKNOWLEDGEMENTS

The project leading to this paper was financed by multiple parties: the Royal Netherlands Navy, MARIN, Wärtsilä Propulsion Netherlands, IMTECH, The Royal Australian Navy, Defence Research and Development Canada, Delft University of Technology, and the Netherlands Defence Academy.

The full scale trials including extensive preparations were made possible by indispensable help, advice and support of the personnel of the Navy Dockyard and CZSK in Den Helder.

The author is further thankful to the crew of HNLMS van Galen, for their vital support, flexibility and hospitality during the intensive trial period.

REFERENCES

Schlesinger, S. (1979). “Terminology for model credibility.” *Simulation*, 32(3):103–104.

Schulten, P. and Stapersma, D. (2007). “A study of the validity of a complex simulation model.” *Journal of Marine Engineering and Technology*, A10:67–77.

van Terwisga, T.; van Wijngaarden, E.; Bosschers, J. and Kuiper, G. (2007). “Achievements and challenges in cavitation research on ship propellers.” *International Shipbuilding Progress*, 54:165-187.

Verkuyl, J. B. and van Terwisga, P. F. (2000). “Testing a new fullscale cavitation observation system on board of Hr. Ms. Tydeman.” *In Proceedings of the 34th WEGEMT School.*

Vrijdag, A., Schulten, P., Stapersma, D., and van Terwisga, T. (2007). “Efficient uncertainty analysis of a complex multidisciplinary simulation model.” *Journal of Marine Engineering and Technology*, A10:79–88.

Vrijdag, A., Stapersma, D., and van Terwisga, T. (2008). “Tradeoffs in ship propulsion control: engine overloading and cavitation inception in operational conditions.” *Proceedings of the 9th International Naval Engineering Conference (INEC2008)*. pp 82-93.

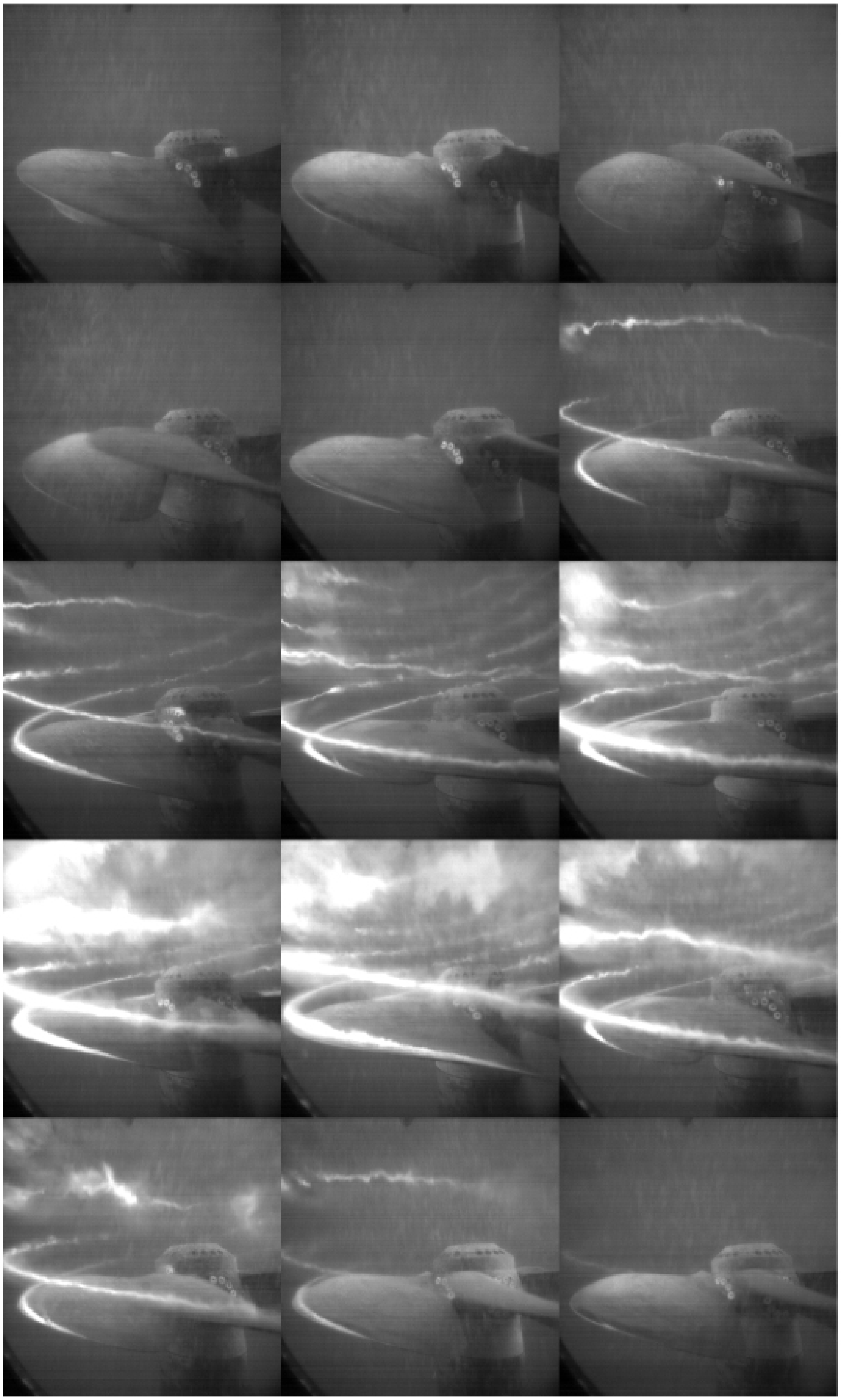

Fig 31: Cavitation behaviour of old PCS, display interval 1s, start at t=540s.

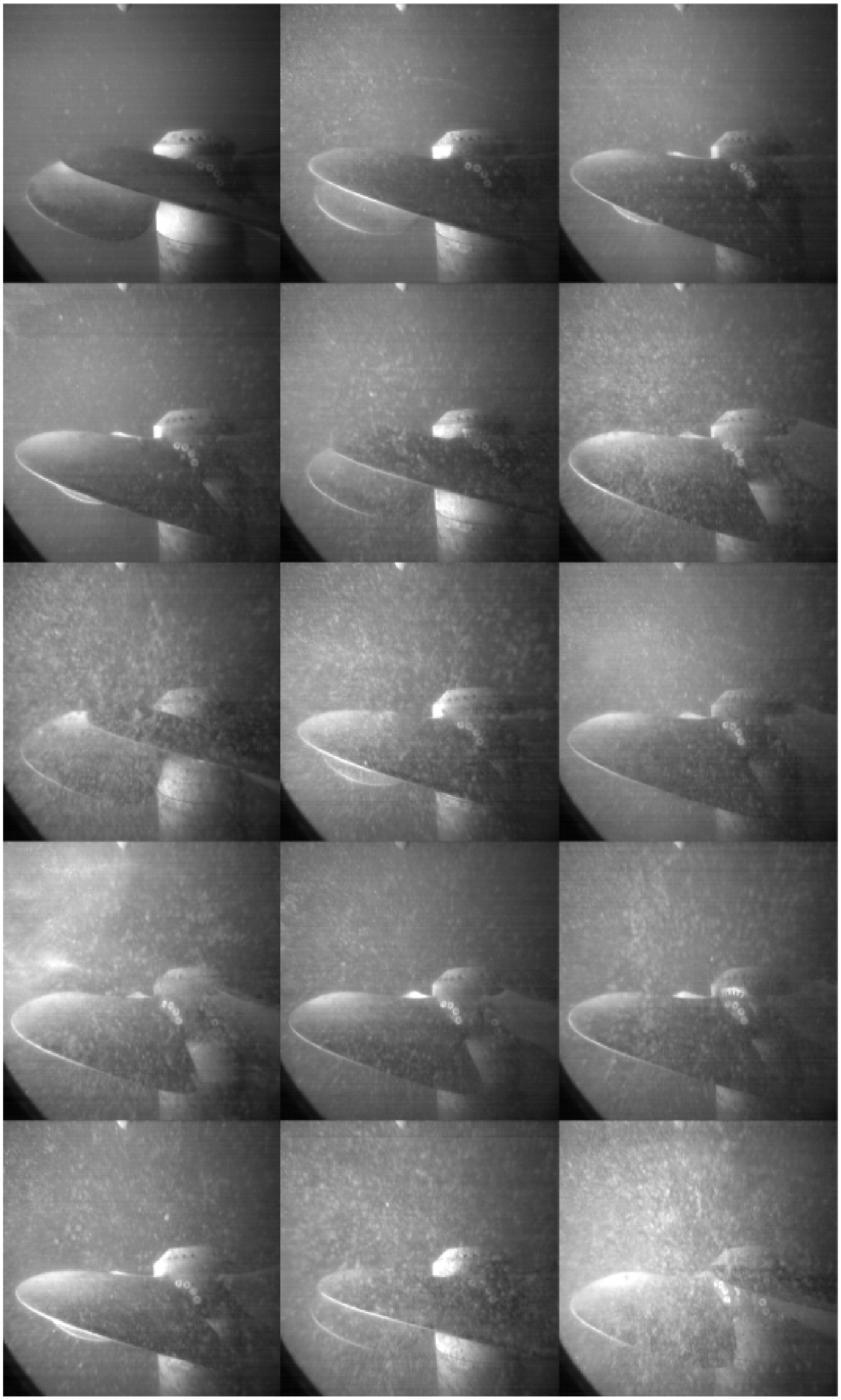

Fig 32: Cavitation behaviour of PCS+, display interval 1s, start at t=543s.